

Ionization-induced azimuthal oscillation in Hall Effect Thrusters

IEPC-2011-196

*Presented at the 32nd International Electric Propulsion Conference,
Wiesbaden, Germany
September 11–15, 2011*

Diego Escobar* and Eduardo Ahedo†
Universidad Politécnica de Madrid (UPM), Madrid, 28040, Spain

In this paper recent results based on a local linear stability analysis of the ionization region a Hall Thruster are presented. A one dimensional azimuthal framework is used including three species: neutrals, singly-charged ions and electrons. A simplified linear model is developed with the aim of deriving analytical expressions that characterize the instability. The results indicate the existence of an instability that gives rise to an azimuthal oscillation with a mode number $m = 1$. According to the model, the instability seems to appear only in regions where the ionization and the electric field make it possible to have positive gradients of plasma density and ion velocity at the same time. A more complex model is also solved numerically to validate the analytical results. Moreover, parametric analyses are carried out with respect to the main parameters of the complex model. As the temperature increases and the neutral-to-plasma density ratio decreases, the growth rate of the instability decreases down to a limit where azimuthal perturbations are no longer unstable. The computation of the eigenvalues and eigenvectors of the linear stability problem shows a correlation between the plasma density and electron axial velocity perturbations. Consequently, a net axial electron current is generated by this oscillation and thus it is possibly linked to anomalous diffusion.

Nomenclature

f_0, \hat{f}	= zero-th order solution and perturbation of macroscopic variable f
\bar{f}	= coefficient of Fourier-like perturbation of variable f
\tilde{f}	= non-dimensional version of variable f or coefficient \bar{f}
i, e, n	= sub-index for ion, electron and neutral species
n, n_n	= plasma and neutral density
\vec{v}_j	= velocity vector of species j
ξ_i, ξ_e	= ionization and electron-neutral collision rates
ν_i, ν_e	= ionization and electron-neutral collision frequencies
e	= electron charge
T_e, \vec{q}_e	= electron temperature and heat conduction flux vector
m_e, m_i, m_n	= electron, ion and neutral masses
\vec{E}, \vec{B}	= electric and magnetic fields
ϕ	= electric potential
$\omega_{i,e}$	= ion and electron cyclotron Larmor frequencies
$\omega k, \lambda$	= frequency, wave number and wavelength of perturbation
l_n	= dimension of the axial variation of plasma density
α_i	= energy loss per actual ionization

*PhD Candidate, Equipo de Propulsión Espacial y Plasmas, <http://web.fmetsia.upm.es/ep2>

†Professor, Equipo de Propulsión Espacial y Plasmas, eduardo.ahedo@upm.es

I. Introduction

Hall Effect Thrusters (HET) are a type of electric propulsion device initially developed in the 1960's by both the USA¹ and the former USSR^{2,3} independently. The development continued in the shadow during the 1970's and 1980's in the USSR to reach a mature status. In the 1990's the advanced state of this Russian technology arrived to western countries, which rapidly restarted the analysis and development of Hall thrusters. Nowadays, there are several companies manufacturing modern Hall thrusters for operational use in USA, Russia and Europe. The main applications of these thrusters are: low-thrust propulsion of interplanetary probes, orbital raising of satellites and north-south station-keeping (NSSK) of geostationary satellites.⁴ There are two basic variants of Hall Thrusters, the stationary plasma thruster (SPTs) and the thruster with anode layer (TAL) in Russian nomenclature. The main difference between them is the material of the walls of the device: ceramic for SPT's and metallic for TAL's. Here we will focus only on the SPT version since it is the most advanced and widely used option.

The operation principle of a typical Hall thruster is as follows. A strong radial magnetic field is imposed together with an axial electric field inside a coaxial chamber where a neutral gas, typically Xenon, is used as propellant. There are three species of particles involved: neutrals, that are injected from the rear part of the channel and flow axially towards the thruster exit; electrons, that are introduced by the cathode located just outside the channel and flow upstream - towards the anode - describing a ExB closed-drift in the azimuthal direction; and ions, that are created by ionization of neutrals due to collisions with the counter-streaming electrons and are accelerated axially by the electric field in the channel and the near plume. The magnetic field is such that electrons are strongly magnetized (i.e., the electron Larmor radius is much smaller than the typical length scale of the thruster) whereas ions are unmagnetized.

Over the last decade great efforts have been dedicated by the HET community to the understanding of the physics of these devices. However, there are still some important aspects to clarify. Since the early stages of the Hall thruster technology development, it has been clear that the electron conductivity inside the chamber and in the plume is too high to be explained with classical collisional theories.⁵ That is why the term anomalous diffusion is used to refer to the higher-than-expected electron current. The radial magnetic field and the axial electric field trap the electrons in an azimuthal closed-drift and, according to classical theory, the only mechanism that allows the electrons to drift axially is the collisions with other species. However, the electron conductivity measured experimentally is two orders of magnitude higher than that expected from collisions. Thus, another mechanism is suspected to enhance the electron mobility.

The main experimentally verified properties of the anomalous diffusion can be summarized as: a) it is present in the whole channel as well as in the plume of the thruster;⁶ b) it is higher outside than inside the channel;⁷ c) there is a dip of electron conductivity⁶⁻⁹ in the region of high magnetic and electric field; d) the electron mobility scales as $1/B$ rather than as $1/B^2$ according to two independent studies;^{10,11} and e) the magnetic field gradients affect greatly the electron conductivity.¹²

Currently there is no agreement within the Hall thruster community about the anomalous diffusion mechanism, but the most accepted explanations are two: plasma oscillations, referred to as Bohm-type diffusion as well as turbulence, based on the fact that correlated azimuthal oscillations of density and electric field can induce a net axial electron current;^{13,14} and near wall conductivity, based on the fact that secondary electrons emitted by the walls introduce a net axial current.¹⁵ However, near wall conductivity does not seem to explain the anomalous diffusion due to the $1/B$ scaling suggested by Boniface *et al.*¹⁰ And many simulation codes¹⁶⁻¹⁸ that introduce near wall conductivity still need Bohm-type diffusion to match the electron conductivity measured experimentally. On the other hand, several experiments have confirmed with various techniques the presence of azimuthal oscillations. These oscillations are normally grouped into low frequency (a few kHz) and high frequency (a few MHz) oscillations. Many linear stability analyses focus on the acceleration region, where the ionization can be safely neglected, and on the high frequency regime. However, experimental results show the presence of low frequency azimuthal oscillations originated in the ionization region of the thruster.^{14,19-21} And precisely, the theoretical analyses of this oscillation, usually called spoke, is the topic of this paper.

The paper is organized as follows. In Section II a review of the available information on low frequency oscillations is presented from three points of view: experiments, numerical simulations and theoretical analyses. A linear stability analysis of azimuthal low frequency perturbations is carried out in Section III. Finally, Section IV is dedicated to conclusions.

II. Review of low frequency azimuthal oscillations in Hall thrusters

A. Experimental results

Back in the 1960's, Janes and Lowder¹⁴ carried out a seminal work on low frequency azimuthal oscillations in HET. Even though the Hall accelerator analysed in that research differs significantly from modern HET, many of the conclusions are still valid. In that study, a spoke was detected by means of azimuthally separated Langmuir probes. This spoke appeared as a density variation rotating azimuthally in the ExB direction with a phase velocity of a few km/s and an axial tilt of 20 degrees. The density variation was phase-correlated with the oscillating electric field and, consequently, the electron axial mobility was enhanced. The phase velocity of the rotating spoke was one order of magnitude smaller than the local ExB drift. Moreover, as part of the research, different propellants were used and it turned out that the phase velocity of the spoke scaled with the ionization potential of the neutral gas: Xenon, Krypton or Argon. All these facts seemed to indicate a close connection between the ionization process and the appearance of the density wave. Janes and Lowder made as well use of the statistical theory of Yoshikawa and Rose¹³ obtaining a very good agreement with the experiments in terms of the anomalous diffusion coefficient. Shortly after, Lomas *et al.*¹⁹ reproduced the experimental results of Janes *et al.* and carried out an analysis of the influence of the magnetic field. According to their analysis, the phase speed of the spoke increases with the magnetic field, an interesting property not mentioned by Janes and Lowder.

Over the last decade several studies have been carried out with modern HET to characterize the low frequency azimuthal oscillations for a wide range of operating conditions and thrusters, both inside and outside the channel. In the first of these analyses, Meezan and Capelli^{6,8,9} use several low-frequency diagnosis methods to measure experimentally the electron mobility along the thruster. The results are in line with the general properties of anomalous diffusion presented above, and in particular, with the presence of a dip in the electron conductivity around the region of maximum electron shear. And what is more important, the electron mobility profile computed from the experimental density oscillations with the theory of Yoshikawa and Rose matches surprisingly well the measured mobility for various operating conditions. A possible correlation between the dip and the electron shear is suggested by Cappelli, although no definitive conclusions have been reached to this respect. A similar mechanism of electron transport barrier due to high electron shear has been proposed in the area of nuclear fusion inside tokamaks,²² although plasmas are in rather different conditions.

In a separate study Chesta *et al.*²⁰ focus on the characterization of all low frequency (LF) oscillations in HET, both axial and azimuthal. In this work, the common breathing mode and transit time oscillations are clearly observable together with some special azimuthal oscillations. The latter ones are caused firstly by the asymmetry of the magnetic field, generated by four magnetic coils, and secondly by the presence of two azimuthally separated Langmuir probes. Apart from those oscillations, two (or possibly one) additional azimuthal low frequency waves with a tilt angle of 15-20 degrees and a mode number of $m = 1$ are detected at low and at high voltage. The oscillation at low voltage has a phase velocity of a few km/s with a frequency of 5-10 kHz and thus seems to match the properties of the rotating spoke detected by Janes and Lowder¹⁴ and by Lomas.¹⁹ On the other hand, the oscillation at high voltage has a frequency of roughly 20 kHz and could be the natural extension of the rotating spoke to the magnetic saturation part of the I-V curve. Moreover, the relative size of the LF density oscillations with respect to the azimuthally averaged density shows a dip in most operating conditions around the region of high magnetic field in agreement with the results obtained by Meezan.

In line with the previous work, Gascon *et al.*²³⁻²⁵ study the propagation properties of LF oscillations and analyse the influence of the ceramic material used: either alumina or boron nitride. In this study, low-to-medium (50-200 kHz) frequency azimuthal and axial oscillations are detected at various axial locations. As in previous studies, azimuthal waves are suppressed around the region of maximum magnetic field. The main novelty is the dependence of the direction of propagation of the azimuthal waves on the ceramic material. The type of material affects the azimuthal wave by controlling the relative position of the magnetic field and density maxima via the secondary electron emission yield of the material.

Smith *et al.*²⁶ analyse the LF variation of density, temperature and electric field in the near field plume of a HET operating in nominal conditions. A density variation is detected at the thruster exit that rotates in the -ExB direction with a phase velocity of 1.8 km/s and a frequency of 25 kHz. The propagation properties of this oscillation agree well with the results previously described, except for the propagation direction which is reported to be opposite to the usual ExB drift.

Very recently, Raitsev *et al.*²⁷ and Parker *et al.*²¹ have discovered spoke instabilities in a cylindrical Hall thruster. In that case, the spoke travels in the ExB direction with a phase speed of about 2 km/s and wave number consistent with a $m = 1$ mode. These properties agree well with other experiments described above. Additionally, the influence of the cathode operation on the spoke and the electron mobility is analysed in that research. In particular, if the cathode emission is increased, the spoke no longer occurs and the electron conductivity is greatly reduced. This is an extremely good indication of the close connection between the anomalous diffusion mechanism and the spoke instability.

The renewed interest in low frequency spoke instabilities is also proven by the two papers of this conference presented by Ellison *et al.*²⁸ and McDonald and Gallimore²⁹ which show experimental evidence of spokes and their relation with the high cross-field electron mobility.

B. Theoretical models: linear stability analyses

The first complete linear stability analysis of the HET discharge was carried out by Esipchuk and Tulinin,³⁰ as a continuation of Morozov's analysis.¹² In Esipchuk's study, the linear stability of a collisionless two-fluid system (electrons and ions) is analysed in the electrostatic regime. LF waves are predicted in locations where the gradient of the magnetic field to density ratio, B/n , is negative. This result is in good agreement with the findings of a more recent analysis by Chesta *et al.*³¹ However, the formulation used in the former study does not include effects such as ionization which are claimed to be very important by Chesta. Moreover, both experimental²⁵ and numerical results³² predict LF waves inside the thruster in regions of positive gradients of B/n . This reinforces the need to revisit the stability against disturbances in the LF regime.

Also in the 1970's, Lomas *et al.*,¹⁹ apart from reproducing the experimental results of Janes and Lowder, carry out a simplified linear stability analysis of the Hall accelerator and suggest the growth of electro-thermal instabilities linked to the spokes detected experimentally. However, the growth mechanism is related to the interaction of ionization and volume recombination, the latter being negligible in modern HET.

Chesta *et al.*³¹ evaluate the linear stability of experimental steady state profiles with a 2D three-fluid description of the discharge including ionization, particle collisions and electromagnetic effects. The main conclusion of that research is that the magnetic field and density gradients together with the ionization define the stability of LF azimuthal waves but no analysis is carried out to unveil the exact mechanism.

Gallardo *et al.*³³ use a three-fluid formalism without electromagnetic terms to analyse the relation of the LF azimuthal waves with the electron anomalous diffusion. The main novelty with respect to previous studies is that the azimuthal three-fluid unsteady equations are solved to observe non-linear saturation effects. The conditions analysed in that case correspond to the ionization region of the channel and the results predict a $m = 3$ azimuthal wave promoted by the ionization process with a phase velocity of 2.7 km/s travelling in the -ExB direction, which is opposite to what is normally observed experimentally. However, there is a flaw in the formulation used since the axial electron velocity is considered constant, what might explain why the computed wave propagates in the direction opposite to experiments.

Kapulkin³⁴ carries out yet another stability analysis specifically suited for the near-anode region where ionization is negligible and the temperature and the magnetic curvature contribute to the azimuthal drift of the electron flow. The results indicate the presence of an unstable wave of low frequency with a non-zero azimuthal component of the wave vector that can promote electron conductivity towards the anode.

C. Numerical simulations

Lomas *et al.*¹⁹ support their experimental results with the numerical solution of a simplified version of the two-dimensional fluid equations for electron, ions and neutrals in a Hall accelerator with Hydrogen as propellant. Even though the conditions of the simulations are far from modern HET, it is interesting to see that low frequency azimuthal oscillations can be promoted by the ionization in a Hall device.

More recently, Lam *et al.*³² have developed a hybrid model that is the natural extension of Fife's hybrid code³⁵ to the $r - \theta$ space. Azimuthal effects are kept in the formulation at the expense of not resolving the radial direction. The preliminary results of this code for the nominal operating point of the simulated thruster show a low frequency (40 kHz) tilted wave with a phase velocity of 4 km/s . This wave propagates in ExB and -z directions inside the channel whereas in the plume the directions of propagation of the wave are reversed. This seems to be correlated with the change in the gradient of the magnetic field. Moreover, in the region of maximum magnetic field the waves are mostly axial as detected experimentally.^{24,25} Unfortunately, the exact mechanism for the growth of these LF waves is not evident from the numerical simulations.

III. Azimuthal linear stability analyses of the ionization region

There is experimental evidence^{14, 19–21, 25, 28, 29} about azimuthal oscillations in the ionization region of the HET discharge. In this region the ionization plays a major role defining the axial profile of the main plasma variables. In order to account for this process, apart from the usual two-fluid ion-electron equations, it is necessary to consider the conservation equations of neutrals and, optionally, an electron energy equation to consider temperature variations.

A. Isothermal model

In a first stage the electron temperature is considered constant ($T_e = \text{const} = T_{e0}$) so that no energy equation is needed. Later on the model will be extended to include an electron energy equation. The current formulation consists of particle and momentum conservation equations for electrons, ions and neutrals separately:

$$\begin{aligned}
\frac{\partial n}{\partial t} + \nabla \cdot (n\vec{v}_e) &= nn_n \xi_i \\
\frac{\partial n}{\partial t} + \nabla \cdot (n\vec{v}_i) &= nn_n \xi_i \\
\frac{\partial n_n}{\partial t} + \nabla \cdot (n_n \vec{v}_n) &= -nn_n \xi_i \\
0 &= -\nabla(nT_e) - en(\vec{E} + \vec{v}_e \times \vec{B}) - m_e nn_n \xi_e \vec{v}_e \\
m_i n \left(\frac{\partial \vec{v}_i}{\partial t} + \vec{v}_i \cdot \nabla \vec{v}_i \right) &= en\vec{E} - m_i nn_n \xi_i (\vec{v}_i - \vec{v}_n) \\
m_n n_n \left(\frac{\partial \vec{v}_n}{\partial t} + \vec{v}_n \cdot \nabla \vec{v}_n \right) &= \vec{0}
\end{aligned} \tag{1}$$

The corresponding steady state zero-th order solution ($\partial/\partial t = 0, \partial/\partial y = 0$) verifies $dn_0/dx > 0$ and $dv_{ix0}/dx > 0$ due to the ionization and the positive zero-th order electric field ($E_{x0} > 0$).

Assuming small perturbations with respect to the zero-th order state, the linearised equations can be written as:

$$\begin{aligned}
\frac{\partial \hat{n}}{\partial t} + n_0 \left(\frac{\partial \hat{v}_{ex}}{\partial x} + \frac{\partial \hat{v}_{ey}}{\partial y} \right) + \hat{v}_{ex} \frac{dn_0}{dx} + v_{ex0} \frac{\partial \hat{n}}{\partial x} + v_{ey0} \frac{\partial \hat{n}}{\partial y} + \hat{n} \frac{dv_{ex0}}{dx} &= (n_0 \hat{n}_n + \hat{n} n_{n0}) \xi_{i0} \\
\frac{\partial \hat{n}}{\partial t} + n_0 \left(\frac{\partial \hat{v}_{ix}}{\partial x} + \frac{\partial \hat{v}_{iy}}{\partial y} \right) + \hat{v}_{ix} \frac{dn_0}{dx} + v_{ix0} \frac{\partial \hat{n}}{\partial x} + \hat{n} \frac{dv_{ix0}}{dx} &= (n_0 \hat{n}_n + \hat{n} n_{n0}) \xi_{i0} \\
\frac{\partial \hat{n}_n}{\partial t} + n_{n0} \left(\frac{\partial \hat{v}_{nx}}{\partial x} + \frac{\partial \hat{v}_{ny}}{\partial y} \right) + \hat{v}_{nx} \frac{dn_{n0}}{dx} + v_{nx0} \frac{\partial \hat{n}_n}{\partial x} &= -(n_0 \hat{n}_n + \hat{n} n_{n0}) \xi_{i0} \\
0 &= -\frac{1}{n_0} \frac{T_{e0}}{m_e} \frac{\partial \hat{n}}{\partial x} + \frac{\hat{n}}{n_0^2} \frac{T_{e0}}{m_e} \frac{dn_0}{dx} - \frac{e}{m_e} \left(-\frac{\partial \hat{\phi}}{\partial x} + \hat{v}_{ey} B_0 \right) - (n_{n0} \hat{v}_{ex} + \hat{n}_n v_{ex0}) \xi_{e0} \\
0 &= -\frac{1}{n_0} \frac{T_{e0}}{m_e} \frac{\partial \hat{n}}{\partial y} - \frac{e}{m_e} \left(-\frac{\partial \hat{\phi}}{\partial y} - \hat{v}_{ex} B_0 \right) - (n_{n0} \hat{v}_{ey} + \hat{n}_n v_{ey0}) \xi_{e0} \\
\frac{\partial \hat{v}_{ix}}{\partial t} + v_{ix0} \frac{\partial \hat{v}_{ix}}{\partial x} + \hat{v}_{ix} \frac{dv_{ix0}}{dx} &= -\frac{e}{m_i} \frac{\partial \hat{\phi}}{\partial x} - n_{n0} \xi_{i0} (\hat{v}_{ix} - \hat{v}_{nx}) - \hat{n}_n \xi_{i0} (v_{ix0} - v_{nx0}) \\
\frac{\partial \hat{v}_{iy}}{\partial t} + v_{ix0} \frac{\partial \hat{v}_{iy}}{\partial x} &= -\frac{e}{m_i} \frac{\partial \hat{\phi}}{\partial y} - n_{n0} \xi_{i0} (\hat{v}_{iy} - \hat{v}_{ny}) \\
\frac{\partial \hat{v}_{nx}}{\partial t} + v_{nx0} \frac{\partial \hat{v}_{nx}}{\partial x} &= 0 \\
\frac{\partial \hat{v}_{ny}}{\partial t} + v_{nx0} \frac{\partial \hat{v}_{ny}}{\partial x} &= 0
\end{aligned} \tag{2}$$

The quasi-neutrality assumption ($n_e = n_i$) has been introduced in the formulation since the Debye length in HET is much smaller than the dimensions of interest for this research. The electron-neutral collision and ionization frequencies have been expressed as $\nu_e = n_n \xi_e$ and $\nu_i = n_n \xi_i$ to make their dependence on the neutral density explicit. In the remainder of the study, it will be assumed that the collision and ionization rates are constant ($\xi_e = \xi_{e0}$, $\xi_i = \xi_{i0}$), even though experiments show a dependence with the electron temperature. Finally, notice as well that the induced magnetic field is neglected and thus, Maxwell's equations are not included in the model. Consequently, the magnetic field is equal to the externally applied field, which is stationary ($\partial \vec{B} / \partial t = 0$), solenoidal ($\nabla \cdot \vec{B} = 0$), irrotational ($\nabla \times \vec{B} = 0$) and mostly radial and the electric field derives from a potential ($\nabla \phi = -\vec{E}$). All this implies that electromagnetic effects are neglected completely and the problem is reduced to an electrostatic formulation.

The perturbations are assumed to be of the form: $\hat{f}(t, y) = \bar{f} \exp(-i\omega t + ik_y y)$. The use of x -independent perturbations is an usual method in the frame of local linear stability analyses in inhomogeneous plasma. For instance, the resistive density-gradient instability is analysed with the same approach by Swanson,³⁶ Chen,³⁷ Miyamoto³⁸ or Krall.³⁹

Given the previous set of equations, it is possible to make the problem non-dimensional by choosing the following reference variables for mass, charge, time, density and length respectively: $m_i = 2.2 \times 10^{-25}$ kg, $e = 1.6 \times 10^{-19}$ C, $\omega_i = eB_0/m_i = 10$ kHz, $n_0 = 5 \times 10^{17}$ m⁻³ and $l_n = -d \ln n_0 / dx = -1$ cm. Even though it might seem strange, a negative reference length is used for consistency with linear stability analyses of the acceleration region where the density gradient is negative and thus l_n is positive.

The non-dimensional version of the resulting linearised equations can be written as an eigenvalue problem in matrix form: $(A\tilde{\omega} + B)\vec{w} = \vec{0}$ where $\vec{w} = (\tilde{n}; \tilde{n}_n; \tilde{v}_{ix}; \tilde{v}_{iy}; \tilde{\phi}; \tilde{v}_{ex}; \tilde{v}_{ey})$. The eigenvalue problem has one unknown ($\tilde{\omega}$), one independent variable (\tilde{k}_y) and a few non-dimensional parameters (\tilde{n}_{n0} , \tilde{v}_{ix0} , \tilde{v}_{nx0} , $\tilde{\xi}_{i0}$, $\tilde{\xi}_{e0}$, \tilde{T}_{e0}). Since the electron inertia and electromagnetic terms have been neglected, no time derivatives of \tilde{v}_{ex} , \tilde{v}_{ey} and $\tilde{\phi}$ appear in the formulation and therefore there are only four solutions for $\tilde{\omega}$ (i.e., three equations can be pre-eliminated in the matrix formulation).

Notice that the perturbations of the neutral velocity are zero ($\tilde{v}_{nx} = \tilde{v}_{ny} = 0$) according to the perturbed neutral momentum equations. And if the following relation is used $\tilde{\nu}_{e0} = \tilde{n}_{n0} \tilde{\xi}_{e0} \ll \tilde{\omega}_e$, it holds that $\tilde{v}_{ex0} = \tilde{v}_{ey0} \tilde{\nu}_{e0} / \tilde{\omega}_e$ and $\tilde{v}_{ey0} = \tilde{T}_{e0} - \tilde{E}_0 = \tilde{T}_{e0} - \tilde{n}_{n0} \tilde{\xi}_{i0} (2\tilde{v}_{ix0} - \tilde{v}_{nx0}) - \tilde{v}_{ix0}^2$ where $\tilde{v}_{ix0} < 0$ since $l_n < 0$.

1. Approximate solution

Let us consider the collision-less limit ($\tilde{\nu}_{e0} = 0$) and equal ion and neutral zero-th order velocities ($\tilde{v}_{nx0} = \tilde{v}_{ix0}$). The second hypothesis is based on the fact that newly created ions have initially the same velocity as the neutrals. Then, it is possible to obtain the following simplified dispersion relation for the eigenvalue problem:

$$0 = (\tilde{\omega} + i\tilde{n}_{n0}\tilde{\xi}_{i0}) \left((\tilde{\omega} + i\tilde{v}_{ix0}) - \frac{\tilde{n}_{n0}\tilde{\xi}_{i0}^2}{\tilde{\omega} + i\tilde{\xi}_{i0}} \right) - \tilde{k}_y \left(\tilde{\omega} - \tilde{k}_y(\tilde{v}_{ey0} - 2\tilde{T}_{e0}) - \frac{\tilde{n}_{n0}\tilde{\xi}_{i0}^2}{\tilde{\omega} + i\tilde{\xi}_{i0}} \right) \quad (3)$$

which reduces to the dispersion relation by Morozov¹² and Esipchuk *et al.*³⁰ in the no-ionization ($\tilde{\xi}_{i0} = 0$), cold electrons ($\tilde{T}_{e0} = 0$) and low frequency ($\tilde{\omega} \ll \tilde{k}_y \tilde{v}_{ey0}$) limit. Equation (3) is cubic in $\tilde{\omega}$ and thus has three solutions. The fourth solution of the general problem comes from the ion momentum equation in the x direction and is a stable solution ($\text{Re}(\tilde{\omega}) > 0$) under the current assumptions.

For typical conditions in the ionization region of a Hall thruster it holds approximately that $\tilde{n}_{n0} \gg 1$, $\tilde{\xi}_{i0} \ll 1$, $\tilde{n}_{n0}\tilde{\xi}_{i0} \sim 1$ and $(-\tilde{v}_{ix0}) \sim 1$. Taking into account those orders of magnitude, Eq.(3) simplifies to:

$$0 = \tilde{\omega}^2 + \tilde{\omega}(i\tilde{n}_{n0}\tilde{\xi}_{i0} + i\tilde{v}_{ix0} - \tilde{k}_y) - (1 + \tilde{k}_y^2)(\tilde{n}_{n0}\tilde{\xi}_{i0}\tilde{v}_{ix0}) - \tilde{k}_y^2(\tilde{v}_{ix0}^2 + \tilde{T}_{e0}) \quad (4)$$

The solutions of Eq.(4) are in the low frequency regime and are unstable under the following condition:

$$\tilde{k}_y^2 < \frac{\tilde{n}_{n0}\tilde{\xi}_{i0}(-\tilde{v}_{ix0})}{\tilde{T}_{e0} + \tilde{E}_0} = \frac{\tilde{n}_{n0}\tilde{\xi}_{i0}(-\tilde{v}_{ix0})}{\tilde{T}_{e0} - \tilde{n}_{n0}\tilde{\xi}_{i0}(-\tilde{v}_{ix0}) + \tilde{v}_{ix0}^2} \quad (5)$$

where it is assumed that $0 < (-\tilde{E}_0) < \tilde{T}_{e0}$. According to condition (5), the highest growth rate is obtained for the smallest wave number, this is, for the perturbation with the longest wavelength allowed by boundary conditions. In the current context, azimuthal continuity imposes a lower limit on the azimuthal wave number. This result is in good agreement with the experimental observations, where a rotating spoke is detected and a wavelength equal to the mean circumference of the thruster.

2. Full numerical solution

The numerical solution of the stability analysis of the isothermal model is presented in Figs.1-5. Several parametric analyses are carried out with respect to various parameters (\tilde{v}_{nx0} , $\tilde{\xi}_{e0}$, \tilde{n}_{n0} and \tilde{T}_{e0}) together with the azimuthal wave number, \tilde{k}_y . In all of them it is possible to observe unstable solutions for low wave numbers in agreement with the findings from the simplistic assumptions of the previous paragraph.

Typical values for the macroscopic variables in the ionization region of a HET are:

- neutral velocity at injection, $v_{nx0} = 500$ m/s;
- neutral density, $n_{n0} = 10^{19}$ m⁻³;
- electron temperature, $T_{e0} = 6$ eV;
- electron-neutral collision frequency, $\nu_{e0} = 10^6$ Hz;
- ionization frequency, $\nu_{i0} = 10^5$ Hz.

The corresponding non-dimensional parameters are: $\tilde{v}_{nx0} = -5$, $\tilde{n}_{n0} = 20$, $\tilde{T}_{e0} = 450$, $\tilde{\nu}_{e0} = 10^2$ and $\tilde{\xi}_{i0} = 0.5$. These parameters define the reference state with respect to which the parametric variations are carried out. It is also interesting to point out that a non-dimensional value of the wave number of $\tilde{k}_y = 0.25$ is equivalent to a wavelength of about 24 cm ($\tilde{\lambda} = 2\pi/\tilde{k}_y$) which is the same as the perimeter of a circumference with a mean radius of 4 cm, a typical value for a modern HET. Thus, $\tilde{k}_y = 0.25$ corresponds to a mode $m = 1$ and wave numbers below that threshold are not possible due to azimuthal continuity. Furthermore, a frequency equal to the reference value (10 kHz) and a wavelength of 24 cm yield a phase velocity of about 2.4 km/s, very similar to the ion acoustic speed and the measured velocity of the spoke, and a propagation in the ExB direction, opposite to the y axis (remember that $l_n < 0$ and thus $\tilde{k}_y > 0$ implies $k_y < 0$). Based on those considerations, an oscillation with non-dimensional frequency $\tilde{\omega}_r = 1$ and wave number $\tilde{k}_y = 0.25$ corresponds approximately to a wave similar to the experimentally observed spoke.

Figure 1 shows the influence of the neutral velocity on the growth rate of the perturbations. Note that previously it was assumed equal neutral and ion zero-th order velocities, but Fig. 1 proves that there are unstable solutions even if that hypothesis is relaxed. And Fig. 2 depicts the variation of the stability region with the electron collisions, which were not included in the approximate solution. The results show that even if a large value of the electron collisions is used, the influence on stability is not very significant. Figure 3 shows the growth rate as a function of \tilde{k}_y and \tilde{n}_{n0} . The smaller the neutral density is, the smaller the range of wave numbers for unstable perturbations. And Fig. 4 shows both the growth rate and frequency of the instability as a function of \tilde{k}_y and \tilde{T}_{e0} . As the electron temperature increases, the range of wave numbers for unstable solutions is reduced. In this case, it is also possible to observe that instabilities exist with a frequency around 10 kHz and a wavelength around 24 cm which, as previously mentioned, correspond to the experimental properties of the spoke.

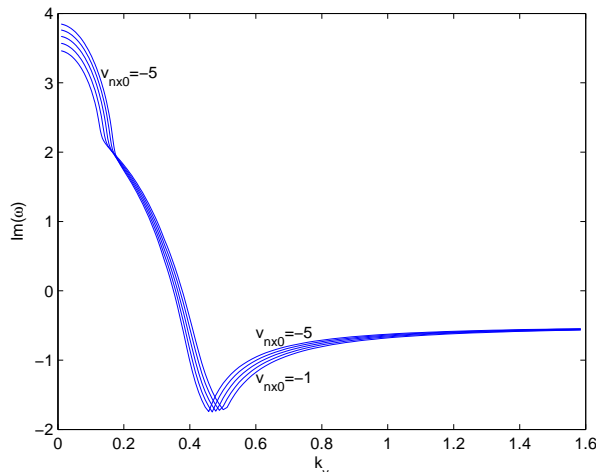


Figure 1. Growth rate of the most unstable solution of (2) for the following non-dimensional parameters: $\tilde{n}_{n0} = 20$, $\tilde{v}_{ix0} = -5$, $\tilde{\xi}_{i0} = 0.5$, $\tilde{\xi}_{e0} = 0$ and $\tilde{T}_{e0} = 450$. Parametric variation of \tilde{k}_y and \tilde{v}_{nx0}

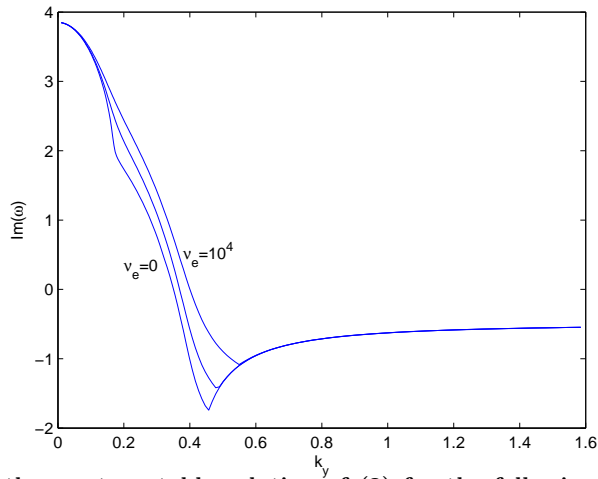


Figure 2. Growth rate of the most unstable solution of (2) for the following non-dimensional parameters: $\tilde{n}_{n0} = 20$, $\tilde{v}_{ix0} = -5$, $\tilde{v}_{nx0} = -5$, $\tilde{\xi}_{i0} = 0.5$ and $\tilde{T}_{e0} = 450$. Parametric variation of k_y and $\tilde{\xi}_{e0}$

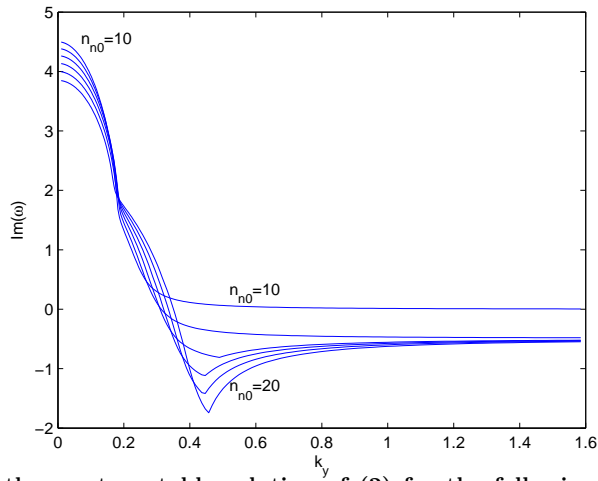


Figure 3. Growth rate of the most unstable solution of (2) for the following non-dimensional parameters: $\tilde{v}_{ix0} = -5$, $\tilde{v}_{nx0} = -5$, $\tilde{\xi}_{i0} = 0.5$, $\tilde{\xi}_{e0} = 0$ and $\tilde{T}_{e0} = 450$. Parametric variation of k_y and \tilde{n}_{n0}

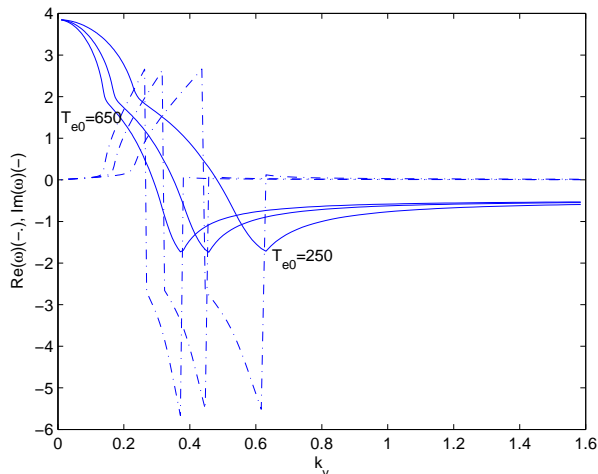


Figure 4. Growth rate (-) and corresponding real part (-) of the most unstable solution of (2) for the following non-dimensional parameters: $\tilde{n}_{n0} = 20$, $\tilde{v}_{ix0} = -5$, $\tilde{v}_{nx0} = -5$, $\tilde{\xi}_{i0} = 0.5$ and $\tilde{\xi}_{e0} = 0$. Parametric variation of k_y and \tilde{T}_{e0}

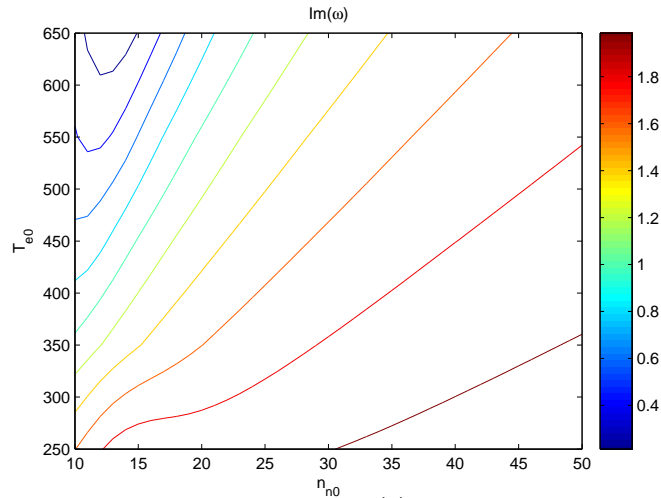


Figure 5. Growth rate of the most unstable solution of (2) for the following non-dimensional parameters: $\tilde{k}_y = 0.25$, $\tilde{v}_{ix0} = -5$, $\tilde{v}_{nx0} = -5$, $\tilde{\xi}_{i0} = 0.5$ and $\tilde{\xi}_{e0} = 0$. Parametric variation of \tilde{n}_{n0} and \tilde{T}_{e0}

Figure 5 depicts a map of the growth rate of the oscillation as a function of the neutral density and the electron temperature for a fixed azimuthal wave number. In our model, as the electron temperature is increased and the neutral-to-plasma density ratio is decreased, the growth rate decreases up to the point where the perturbation is no longer unstable. Experiments show that as the discharge voltage is increased, keeping the rest of parameters constant, the intensity of low frequency oscillations diminishes considerably specially in the ionization part of the I-V curve of the thruster.^{40,41} A discharge voltage increase causes the electron temperature to increase in the ionization region of the thruster via ohmic heating and the neutral-to-plasma density ratio to decrease thanks to improved ionization. Thus, the linear model is in line with the experimental trend.

So far we have only detected unstable oscillations due to the ionization. However, no connection has been established between this instability and enhanced mobility. Looking at the equations in (2), it is possible to recognize that the terms $\tilde{v}_{ex} dn_0/dx$ and $(e/m_e)\tilde{v}_{ex}B_0$ - associated to the perturbation \tilde{v}_{ex} - from the electron continuity and momentum equations play two roles: first, they couple the plasma density fluctuations from the ion equations with the electron momentum equations thanks to the presence of the zero-th order plasma density gradient in the electron continuity equation; and second and more important, it ensures that the azimuthal electric field and plasma density perturbations are correlated giving rise to a net axial current. This second fact can be shown more clearly by computing the phase of the different perturbations numerically. A similar explanation is proposed by Lomas *et al.*¹⁹ with a model that includes an energy equation without heat conduction, although in that case the instability is fed by the coupling between ionization and bulk recombination rather than by the interaction between ionization and the plasma density gradient.

Table 1 shows the eigenvectors of the eigenvalue problem for the following parameters: $\tilde{k}_y = 0.25$, $\tilde{n}_{n0} = 20$, $\tilde{v}_{ix0} = -5$, $\tilde{v}_{nx0} = -5$, $\tilde{\xi}_{i0} = 0.5$, $\tilde{\xi}_{e0} = 0$ and $\tilde{T}_{e0} = 450$. It is very interesting to see how the plasma density and electron axial velocity perturbations are correlated, this is, their phases are not 90 degrees apart, meaning that the unstable oscillation causes a net axial electron current. This is a good indication of anomalous diffusion caused by the azimuthal oscillation.

Table 1. Complex eigenvalues of the stability analysis of (2) for the following non-dimensional parameters: $\tilde{k}_y = 0.25$, $\tilde{n}_{n0} = 20$, $\tilde{v}_{ix0} = -5$, $\tilde{v}_{nx0} = -5$, $\tilde{\xi}_{i0} = 0.5$, $\tilde{\xi}_{e0} = 0$ and $\tilde{T}_{e0} = 450$.

\tilde{n}	\tilde{n}_n	\tilde{v}_{ix}	\tilde{v}_{iy}	$\tilde{\phi}$	\tilde{v}_{ex}	\tilde{v}_{ey}
$0.10\angle -109^\circ$	$0.37\angle 115^\circ$	$0\angle 0^\circ$	$0.88\angle 171^\circ$	$40.4\angle -107^\circ$	$0.60\angle -43^\circ$	$42.6\angle 71^\circ$

B. Simplified model

The dispersion relation in Eq.(4) is equivalent to the following linearised system of perturbation equations in non-dimensional form:

$$\begin{aligned}
\frac{\partial \tilde{n}}{\partial \tilde{t}} + \frac{\partial \tilde{v}_{ey}}{\partial \tilde{y}} - \tilde{v}_{ex} + \tilde{v}_{ey0} \frac{\partial \tilde{n}}{\partial \tilde{y}} &= 0 \\
\tilde{v}_{ey} &= -\tilde{n} \tilde{T}_{e0} \\
0 &= \tilde{T}_{e0} \frac{\partial \tilde{n}}{\partial \tilde{y}} - \frac{\partial \tilde{\phi}}{\partial \tilde{y}} - \tilde{v}_{ex} \\
\frac{\partial \tilde{n}}{\partial \tilde{t}} + \frac{\partial \tilde{v}_{iy}}{\partial \tilde{y}} + \tilde{n} \tilde{v}_{ix0} &= 0 \\
\frac{\partial \tilde{v}_{iy}}{\partial \tilde{t}} + \frac{\partial \tilde{\phi}}{\partial \tilde{y}} + \tilde{n}_{n0} \tilde{\xi}_{i0} \tilde{v}_{iy} &= 0
\end{aligned} \tag{6}$$

Notice that the ionization terms are compensated by the gradients of the zero-th order solution and this explains why there are no source terms in the continuity equations.

If all equations in (6) are combined in one equation for the non-dimensional plasma density, the result is:

$$0 = \frac{\partial^2 \tilde{n}}{\partial \tilde{t}^2} + \frac{\partial^2 \tilde{n}}{\partial \tilde{t} \partial \tilde{y}} + (\tilde{v}_{ey0} - 2\tilde{T}_{e0}) \frac{\partial^2 \tilde{n}}{\partial \tilde{y}^2} + \tilde{n}_{n0} \tilde{\xi}_{i0} \left(\frac{\partial \tilde{n}}{\partial \tilde{t}} + \tilde{n} \tilde{v}_{ix0} \right) + \tilde{v}_{ix0} \frac{\partial \tilde{n}}{\partial \tilde{y}} \tag{7}$$

Since $\tilde{v}_{ey0} - 2\tilde{T}_{e0} < 0$, equation (7) contains a wave-like term ($\partial^2 \tilde{n} / \partial \tilde{y}^2$) whose coefficient ($-\tilde{c}^2$) = $\tilde{v}_{ey0} - 2\tilde{T}_{e0} = -(\tilde{T}_{e0} + \tilde{E}_0) < 0$ corresponds to a wave velocity, $\tilde{c} = \sqrt{\tilde{T}_{e0} + \tilde{E}_0} \approx \sqrt{\tilde{T}_{e0}}$, of the order of the ion acoustic speed. Moreover, the destabilizing element in equation (7) corresponds to the term $\tilde{n} \tilde{n}_{n0} \tilde{\xi}_{i0} (-\tilde{v}_{ix0})$ which is associated to the ionization and the coupling between the continuity and momentum equations of the ion species.

However, the solution of the eigenvalue problem associated to Eqs.(6) (i.e., the analytical approximate solution presented above) indicates that, even though there are unstable perturbations ($\text{Im}(\tilde{\omega}) > 0$), the phase speed of the oscillations is very close to zero ($\text{Re}(\tilde{\omega}) \approx 0$). The reason for this is that in the approximation too many terms have been neglected, in particular, the variation of neutral density. If neutral density oscillations are reintroduced in the previous system, the resulting set of linearised non-dimensional equations can be written as:

$$\begin{aligned}
\frac{\partial \tilde{n}}{\partial \tilde{t}} + \frac{\partial \tilde{v}_{ey}}{\partial \tilde{y}} - \tilde{v}_{ex} + \tilde{v}_{ey0} \frac{\partial \tilde{n}}{\partial \tilde{y}} &= \tilde{n}_n \tilde{\xi}_{i0} \\
\tilde{v}_{ey} &= -\tilde{n} \tilde{T}_{e0} \\
0 &= \tilde{T}_{e0} \frac{\partial \tilde{n}}{\partial \tilde{y}} - \frac{\partial \tilde{\phi}}{\partial \tilde{y}} - \tilde{v}_{ex} \\
\frac{\partial \tilde{n}}{\partial \tilde{t}} + \frac{\partial \tilde{v}_{iy}}{\partial \tilde{y}} + \tilde{n} \tilde{v}_{ix0} &= \tilde{n}_n \tilde{\xi}_{i0} \\
\frac{\partial \tilde{v}_{iy}}{\partial \tilde{t}} + \frac{\partial \tilde{\phi}}{\partial \tilde{y}} + \tilde{n}_{n0} \tilde{\xi}_{i0} \tilde{v}_{iy} &= 0 \\
\frac{\partial \tilde{n}_n}{\partial \tilde{t}} &= -(\tilde{n} \tilde{n}_{n0} + \tilde{n}_n) \tilde{\xi}_{i0}
\end{aligned} \tag{8}$$

Eqs.(8) represent the minimal linear system of equations capable of reproducing the results from the full solution of the eigenvalue problem given by Eqs.(2) in terms of phase speed and growth rate of the unstable perturbations for typical HET conditions. The dispersion relation given by Eq.(3) is equivalent to Eqs.(8).

C. Model with energy equation and heat conduction

In previous sections, a simplified analysis has been carried out accounting for the ionization process in the stability analysis. However, the electron temperature was considered constant and no energy equation was included in the formulation. In this section, both assumptions are relaxed in order to check whether the instability detected with the simplified model still appears with a more complex model. Nevertheless, electron inertia terms and plasma non-quasi-neutrality are still neglected since they are not believed to influence the low frequency instability under analysis.

In this case, no analytical solution is investigated and only the results from the numerical solution of the corresponding eigenvalue problem is shown. Under the previous hypothesis, the governing conservation laws in Eqs.(1) can be extended to account for electron temperature variations with an electron energy conservation equation and a diffusive model of heat conduction flux, \vec{q}_e :

$$\begin{aligned} \frac{\partial}{\partial t} \left(\frac{3}{2} n T_e \right) + \nabla \cdot \left(\frac{5}{2} n T_e \vec{v}_e + \vec{q}_e \right) &= -en\vec{v}_e \cdot \vec{E} - enn_n \xi_i \alpha_i \\ \frac{5}{2} n T_e \nabla T_e + e\vec{q}_e \times \vec{B} + m_e n_n \xi_e \vec{q}_e &= \vec{0} \end{aligned} \quad (9)$$

In order to close the formulation, a hypothesis about the temperature gradient is needed. In this case, an adequate choice seems to be assuming a constant zero-th order temperature axial profile, $dT_{e0}/dx = 0$, as suggested by Gallardo *et al.*,³³ or a linearly varying profile, $d^2T_{e0}/dx^2 = 0$.

After the linearisation of the equations, the use of a Fourier-like form for the perturbations and the transformation to non-dimensional space, the stability analysis can be formulated as an eigenvalue problem, $(A\tilde{\omega} + B)\vec{w} = \vec{0}$ where $\vec{w} = (\tilde{n}; \tilde{n}_n; \tilde{v}_{ix}; \tilde{v}_{iy}; \tilde{\phi}; \tilde{v}_{ex}; \tilde{v}_{ey}; \tilde{T}_e; \tilde{q}_{ex}; \tilde{q}_{ey})$, to solve for the complex frequency of the perturbations, $\tilde{\omega}$. The non-dimensional azimuthal wave number, \tilde{k}_y , is the independent variable of the formulation and the non-dimensional parameters to consider are: \tilde{n}_{n0} , \tilde{v}_{ix0} , \tilde{v}_{nx0} , $\tilde{\xi}_{i0}$, $\tilde{\xi}_{e0}$, \tilde{T}_{e0} and $\tilde{\alpha}_{i0}$. Once again, since no electromagnetic terms and no electron inertia are considered, electron momentum and Poisson's equations together with the heat flux vector can be pre-eliminated in the matrix formulation.

Figure 6 and 7 show the numerical solution of the stability problem for the same case as for the isothermal model. In particular, the growth rate of the most unstable solution and the corresponding real part are depicted in Fig. 6. It is possible to see that the same long-wavelength instability appears as in the isothermal model. Moreover, results from the simpler model are recovered if no temperature gradients are assumed for the zero-th order solution. As the temperature gradient increases, its effect is to reduce the range of azimuthal wave numbers where unstable perturbations exist. On the other hand, the phase speed of the unstable perturbation is still of the order of the ion acoustic speed and the frequency of the oscillation of the order of 10 kHz. Figure 7 shows the stability map of the perturbation with respect to the temperature and the neutral-to-plasma density ratio. The conclusions are similar to the isothermal model.

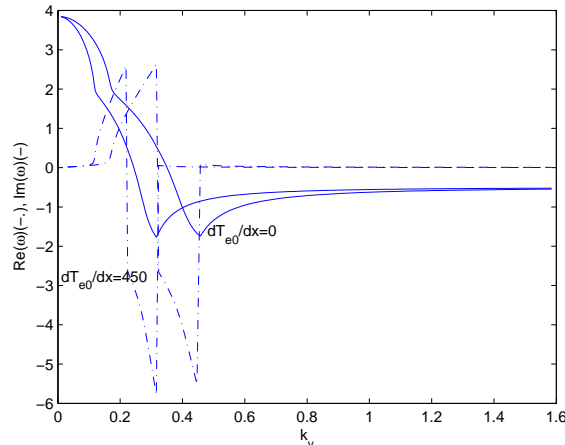


Figure 6. Growth rate (-) and corresponding real part (-) of the most unstable solution of (9) for the following non-dimensional parameters: $\tilde{n}_{n0} = 20$, $\tilde{v}_{ix0} = -5$, $\tilde{v}_{nx0} = -5$, $\tilde{\xi}_{i0} = 0.5$, $\tilde{\xi}_{e0} = 0$ and $\tilde{T}_{e0} = 450$. Parametric variation of \tilde{k}_y and $d\tilde{T}_{e0}/dx$

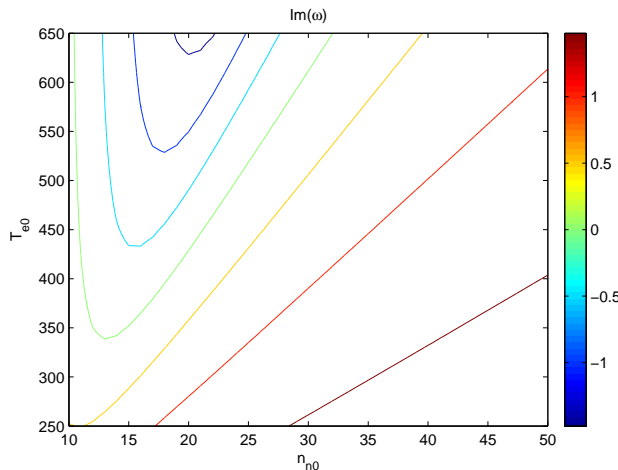


Figure 7. Growth rate of the most unstable solution of (9) for the following non-dimensional parameters: $\bar{k}_y = 0.25$, $\bar{v}_{ix0} = -5$, $\bar{v}_{nx0} = -5$, $\xi_{i0} = 0.5$ and $\xi_{e0} = 0$. Parametric variation of \bar{n}_{n0} and $\bar{T}_{e0} = d\bar{T}_{e0}/d\bar{x}$

IV. Conclusions

A linear stability analysis of the plasma in the ionization region of a Hall Effect thruster has allowed identifying an azimuthal instability which enhances the electron conductivity. The linear instability is very similar to spoke measured experimentally in terms of frequency range and phase speed. Moreover, a simplified set of linear equations able to reproduce completely the instability has been derived. This model must include both source terms due to ionization as well as neutral density variations in order to reproduce the main features of the instability as derived from the full numerical solution of the eigenvalue problem.

However, there are important limitations of the current analysis that recommend extending the work. A first extension would be the consideration of x gradients in the perturbations. Instead of a Fourier expansion, due to the inhomogeneity of the zero-th order solution in the x direction, it is more consistent to keep the dependence on the perturbations. The resulting system of equations is not an algebraic, but a differential eigenvalue problem. Similar approaches have been used by Kapulkin⁴² and Litvak *et al.*⁴³ in the past for other stability studies of the Hall thruster discharge. A second possible extension of the work consists on the resolution of the complete non-linear equations consistent with the simplified isothermal model of the instability. In this way, possible non-linear saturation effects can be recovered.

Acknowledgments

The authors want to thank F.I. Parra for fruitful discussions. The work of E. Ahedo was sponsored by the Gobierno de España (Project No. AYA2010-16699).

References

- ¹G.L. Cann and G.L. Marlotte. Hall current plasma accelerator. *AIAA Journal*, 2(7):1234–1241, 1964.
- ²A.V. Zharinov and Y.S. Popov. Acceleration of plasma by a closed Hall current. *Soviet Physics-Technical Physics*, 12(2):208–211, 1967.
- ³A.I. Morozov, A.Y. Kislov, and I.P. Zubkov. Strong-current Plasma Accelerator with Closed Electron Drift. *ZhETF Pis ma Redaktsiiu*, 7:224–227, 1968.
- ⁴M. Martinez-Sanchez and J.E. Pollard. Spacecraft electric propulsion-an overview. *Journal of Propulsion and Power*, 14(5), 1998.
- ⁵A.I. Morozov, Y.V. Esipchuk, G.N. Tilinin, A.V. Trofimov, and Y.A. Sharov. Plasma accelerator with closed electron drift and extended acceleration zone. *Soviet Physics-Tech. Physics*, 17(1):38–45, 1972.
- ⁶N.B. Meezan and M.A. Cappelli. Electron density measurements for determining the anomalous electron mobility in a coaxial Hall discharge plasma. In *Proceedings of the 36th Joint Propulsion Conference*, 2000.
- ⁷J. A. Linnell and A. D. Gallimore. Hall Thruster Electron Motion Characterization Based on Internal Probe Measurements. In *Proceedings of the 31st International Electric Propulsion Conference*, 2009.
- ⁸N.B. Meezan, W.A. Hargus Jr, and M.A. Cappelli. Anomalous electron mobility in a coaxial Hall discharge plasma. *Physical Review E*, 63(2):26410, 2001.

- ⁹M.A. Cappelli, N.B. Meezan, and N. Gascon. Transport physics in Hall plasma thrusters. In *Proceedings of the 40th AIAA Aerospace and Sciences Meeting and Exhibit*, 2002.
- ¹⁰C. Boniface, L. Garrigues, G.J.M. Hagelaar, J.P. Boeuf, D. Gawron, and S. Mazouffre. Anomalous cross field electron transport in a Hall effect thruster. *Applied Physics Letters*, 89:161503, 2006.
- ¹¹D. Gawron, S. Mazouffre, and C. Boniface. A Fabry–Pérot spectroscopy study on ion flow features. *Plasma Sources Science and Technology*, 15:757–764, 2006.
- ¹²A.I. Morozov, Y.V. Esipchuk, A.M. Kapulkin, V.A. Nevrovskii, and V.A. Smirnov. Effect of the magnetic field on a closed-electron-drift accelerator. *Soviet Physics-Tech. Physics*, 17(3):482–487, 1972.
- ¹³S. Yoshikawa and D.J. Rose. Anomalous diffusion of a plasma across a magnetic field. *Physics of Fluids*, 5:334, 1962.
- ¹⁴G.S. Janes and R.S. Lowder. Anomalous Electron Diffusion and Ion Acceleration in a Low-Density Plasma. *Physics of Fluids*, 9:1115, 1966.
- ¹⁵AI Morozov. Conditions for efficient current transport by near-wall conduction. *Sov. Phys. Tech. Phys*, 32(8):901–904, 1987.
- ¹⁶E. Ahedo, J.M. Gallardo, and M. Martinez-Sanchez. Effects of the radial plasma-wall interaction on the hall thruster discharge. *Physics of Plasmas*, 10:3397, 2003.
- ¹⁷L. Garrigues, G.J.M. Hagelaar, C. Boniface, and J.P. Boeuf. Anomalous conductivity and secondary electron emission in Hall effect thrusters. *Journal of Applied Physics*, 100:123301, 2006.
- ¹⁸F.I. Parra, E. Ahedo, J.M. Fife, and M. Martinez-Sanchez. A two-dimensional hybrid model of the Hall thruster discharge. *Journal of Applied Physics*, 100:023304, 2006.
- ¹⁹P.J. Lomas and J.D. Kilkenny. Electrothermal instabilities in a Hall accelerator. *Plasma Physics*, 19:329, 1977.
- ²⁰E. Chesta, C.M. Lam, N.B. Meezan, D.P. Schmidt, and M.A. Cappelli. A characterization of plasma fluctuations within a Hall discharge. *IEEE transactions on plasma science*, 29(4):582–591, 2001.
- ²¹J.B. Parker, Y. Raitses, and N.J. Fisch. Transition in electron transport in a cylindrical hall thruster. *Applied Physics Letters*, 97:091501, 2010.
- ²²A. Dinklage, T. Klinger, G. Marx, and L. Schweikhard. *Plasma physics: confinement, transport and collective effects*. Berlin Springer Verlag, 2005.
- ²³N. Gascon, N.B. Meezan, and M.A. Cappelli. Low frequency plasma wave dispersion and propagation in Hall thrusters. In *Proceedings of the 27th International Electric Propulsion Conference*, 2001.
- ²⁴N. Gascon and M.A. Capelli. Wall effects on the excitation and propagation of instabilities in Hall thrusters. In *Proceedings of the 28th International Electric Propulsion Conference*, 2003.
- ²⁵N. Gascon and M.A. Cappelli. Plasma instabilities in the ionization regime of a Hall thruster. In *Proceedings of the 29th Joint Propulsion Conference*, 2003.
- ²⁶A.W. Smith and M.A. Cappelli. Time and Space-correlated Plasma Property Measurements in the Near-field of a Coaxial Hall Discharge. In *Proceedings of the 31st International Electric Propulsion Conference*, 2009.
- ²⁷Y. Raitses, A. Smirnov, and N.J. Fisch. Effects of enhanced cathode electron emission on hall thruster operation. *Physics of Plasmas*, 16:057106, 2009.
- ²⁸C. L. Ellison, Y. Raitses, and N. J. Fisch. Direct measurement of spoke-induced, cross-field electron current in a cylindrical Hall thruster. In *Proceedings of the 32nd International Electric Propulsion Conference*, 2011.
- ²⁹M. S. McDonald and D. Gallimore, A. Cross-Field Electron Transport due to Rotating Spoke Instabilities in Hall Thrusters. In *Proceedings of the 32nd International Electric Propulsion Conference*, 2011.
- ³⁰Y.B. Esipchuk and G.N. Tulinin. Drift instability in a Hall-current plasma accelerator. *Sov. Physics-Tech. Physics*, 21(4):417–423, 1976.
- ³¹E. Chesta, N.B. Meezan, and M.A. Cappelli. Stability of a magnetized Hall plasma discharge. *Journal of Applied Physics*, 89(6):3099–3107, 2001.
- ³²C. M. Lam, A. K. Knoll, M. A. Cappelli, and E. Fernandez. Two-Dimensional (z - θ) Simulations of Hall Thruster Anomalous Transport. In *Proceedings of the 31st International Electric Propulsion Conference*, 2009.
- ³³J.M. Gallardo and E. Ahedo. On the anomalous diffusion mechanism in Hall-effect thrusters. In *Proceedings of 29th International Electric Propulsion Conference*, 2005.
- ³⁴A. Kapulkin and M. Guelman. Low Frequency Instability and Enhanced Transfer of Electrons in Near-Anode Region of Hall Thruster. In *Proceedings of the 30th International Electric Propulsion Conference*, 2007.
- ³⁵J.M. Fife. *Hybrid-PIC modelling and electrostatic probe survey of Hall thrusters*. PhD thesis, Massachusetts Institute of Technology, 1998.
- ³⁶D.G. Swanson. *Plasma waves*. Taylor & Francis, 2003.
- ³⁷F.F. Chen. *Introduction to plasma physics and controlled fusion*. Springer, 1984.
- ³⁸K. Miyamoto. *Fundamentals of Plasma Physics and Controlled Fusion*. Iwanami Book Service Center, 1997.
- ³⁹N. A. Krall and A. W. Trivelpiece. *Principles of plasma physics*. McGraw-Hill, 1973.
- ⁴⁰E.Y. Choueiri. Plasma oscillations in Hall thrusters. *Physics of Plasmas*, 8:1411, 2001.
- ⁴¹G.N. Tulinin. High-frequency plasma waves in a Hall accelerator with an extended acceleration zone. *Soviet Physics-Technical Physics*, 22(8):974–978, 1977.
- ⁴²A. Kapulkin, J. Ashkenazy, A. Kogan, G. Appelbaum, D. Alkalay, and M. Guelman. Electron instabilities in Hall thrusters: modelling and application to electric field diagnostics. In *Proceedings of the 28th International Electric Propulsion Conference*, 2003.
- ⁴³A.A. Litvak and N.J. Fisch. Rayleigh instability in Hall thrusters. *Physics of Plasmas*, 11:1379, 2004.